

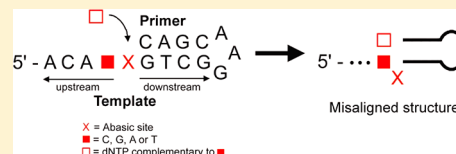
## Effect of an Abasic Site on Strand Slippage in DNA Primer-Templates

Ring Yan Au, Kui Sang Ng, Lai Man Chi, and Sik Lok Lam\*

Department of Chemistry, The Chinese University of Hong Kong, Shatin, New Territories, Hong Kong

## S Supporting Information

**ABSTRACT:** An abasic site is the most common lesion in DNA. It is also an intermediate product formed during base excision repair. Previously, we demonstrated that strand slippage can occur in primer-template model systems containing any kind of natural templating bases, suggesting deletion and expansion errors are possible in any kind of sequences during DNA replication. In this study, nuclear magnetic resonance spectroscopic investigations have been performed to study the intrinsic effect of a templating abasic residue on strand slippage in primer-template models. A DNA hairpin model system containing an abasic site and a 5'-overhang region was used to mimic the situation that a dNTP has just been incorporated opposite the abasic site. Our results show that, after dNTP incorporation, strand slippage occurs regardless of the type of terminal base pair formed. Compared to natural templating bases, abasic sites possess a higher slippage propensity, implicating a higher chance of expansion or deletion errors during DNA replication.



## ■ INTRODUCTION

An abasic site, also known as an apurinic/apyrimidinic (AP) site, is the most frequently found lesion in DNA due to direct spontaneous depurination in physiological condition<sup>1,2</sup> or as an intermediate product in base excision repair (BER).<sup>3–6</sup> Approximately 10 000 AP sites are generated every day in mammalian cells.<sup>1</sup> They present strong blocks to DNA replication, but Y-family translesion polymerases can bypass them, thus leading to a wide range of highly mutagenic products and affecting the fidelity of DNA replication.<sup>7,8</sup>

Although it is important to maintain genetic information over many generations, mutations are sometimes required for evolution of species.<sup>9</sup> Recent advances in studying the fidelity of DNA replication lead us to realize the enormous complexity of the cellular machinery devoted to replicating DNA.<sup>10</sup> We now recognize that the replication fidelity in vivo is a very complicated issue and cannot be determined by a single type of DNA polymerases.<sup>11</sup> In order to replicate both undamaged and damaged DNA, many DNA polymerases are known to exist. At present, at least 16 DNA polymerases have been identified in human cells, including three A-, four B-, four X-, and four Y-family polymerases and one reverse transcriptase.<sup>12</sup> Y-family polymerase is mainly responsible for replicating damaged DNA. It does not have a proofreading activity, but it has an open and solvent accessible active site which allows lesion bypass.<sup>13,14</sup> As a result, the presence of AP sites in templates requires the switching of polymerases during DNA replication.<sup>12</sup>

Earlier efforts have been made in studying the effect of AP residues on the replication products by a single type DNA polymerase.<sup>15–18</sup> These studies improve our understandings of the effect of AP sites on the fidelity of DNA replication. However, these results are polymerase-specific and the intrinsic effect of AP sites on primer-template structures remains unclear. The influence of AP site on DNA structures and replication fidelity has also been extensively investigated through solution structure studies of a number of DNA

duplexes containing an AP site.<sup>15,19–29</sup> These studies showed that AP sites induced only local perturbations in B-DNA. The AP site was extrahelical when the duplex contained a pyrimidine<sup>21,26</sup> or no base<sup>19,20</sup> opposite it but intrahelical when the opposite base became a purine.<sup>15,22–25,27</sup> The AP site was more perturbed structurally when its opposite base was a pyrimidine instead of a purine.<sup>28,29</sup> Nevertheless, all these studies were performed with the AP residue constrained between two flanking double helices and thereby the influence of AP residue on the replicating site structure of primer-templates remains elusive.

In the past decade, as Y-family polymerase has been suggested to play roles in replicative bypass across many DNA lesions, it becomes more important to investigate the effect of AP site on the replication products by Y-family polymerase.<sup>8,15</sup> Owing to the spacious active site of Y-family polymerase and the involvement of polymerase switching in replicating lesions, the intrinsic effect of AP site on the replicating site structures of primer-templates may therefore play a significant role in determining the DNA replication fidelity in vivo. Previously, we performed nuclear magnetic resonance (NMR) structural investigations on primer-template oligonucleotide models that mimic the situation in which a dNTP has just been incorporated opposite different types of templates. We determined that strand slippage can occur in primer-templates containing any kind of templating bases.<sup>30–34</sup> Pending on the direction of replication, strand slippage can lead to expansion or deletion errors during DNA replication.<sup>35,36</sup> Besides, templating purine<sup>30,31</sup> has been found to be less prone to strand slippage than templating pyrimidine.<sup>32–34</sup> As a result, we hypothesize that the larger the templating base size at the replicating site provides better stacking interactions with its

Received: September 4, 2012

Revised: November 27, 2012

Published: December 5, 2012

neighboring bases and thus minimizing strand slippage in primer-templates. For example, substitution of a purine with a pyrimidine at the replicating site leads to a decrease in the base size, and thus an increase in the slippage propensity of the primer-template. Upon base excision at the replicating site, we speculate that the resulting AP site will further enhance the propensity of strand slippage. In order to test our hypothesis, we have performed a systematic NMR study on primer-template models containing an AP residue at the replicating site with different upstream bases in this study. Our results show that the presence of AP sites in templates increases the propensity of strand slippage in primer-templates, providing insights into the adverse effect resulting from the intermediate product of BER during DNA replication.

## EXPERIMENTAL METHODS

**Sample Design.** Four 17-nucleotide DNA sequences containing an AP residue were designed to form primer-template models (Figure 1a). In these models, the AP residue

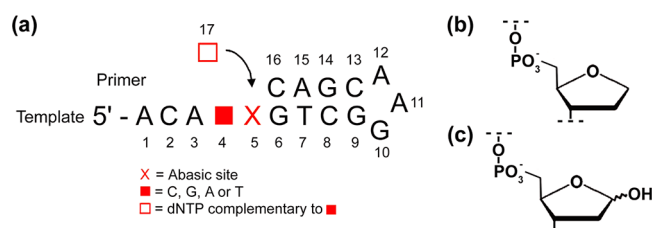


**Figure 1.** (a) The 17-nucleotide primer-template model used in this study. Chemical structures of the (b) tetrahydrofuran abasic analogue and (c) natural abasic site.

was placed at the replicating site of the template strand and labeled as “X” in the sequences. The 5'-overhang regions represent the template sequences, including 5'-ACACX, 5'-ACAGX, 5'-ACAAX, and 5'-ACATX. Each of them contains four residues upstream of X, and the 5'-ACA terminus has been shown to have no effect on the formation of misaligned structures.<sup>32</sup> In order to simplify the sample preparative work, a 5'-GAA loop<sup>37</sup> was used to connect the primer and template strands. The 3'-termini of primer strands mimic the situations that a dGTP, dCTP, dTTP, and dATP has just been incorporated opposite to the AP site of the 5'-ACACX, 5'-ACAGX, 5'-ACAAX, and 5'-ACATX templates, respectively. For simplicity, these primer-template models were named “5'-CX”, “5'-GX”, “5'-AX”, and “5'-TX”, respectively.

For the AP site, a tetrahydrofuran (THF) analogue (Figure 1b) was used instead of a natural AP residue (Figure 1c) because natural AP residues were unstable and feasibly converted to an aldehyde form<sup>19,28</sup> which was subjected to  $\beta$ -elimination and strand scission.<sup>38</sup> Similar extents of 1- and 2-deletion errors had been observed in templates using the natural AP residue and the THF analogue, suggesting they play a similar role in DNA strand slippage.<sup>16,17</sup> In addition, the use of the THF analogue had been validated by the results that it could be efficiently cleaved by major AP endonuclease, and serve as a template for DNA polymerases.<sup>39–44</sup>

**Sample Preparation.** All DNA samples were synthesized using an Applied Biosystems model 394 DNA synthesizer and purified with denaturing polyacrylamide gel electrophoresis and diethylaminoethyl Sephacel anion exchange column chromatography. The AP residue was incorporated into the sequence using an abasic phosphoramidite (ChemGenes, Inc.). Instead of

25 s, an extended period of 600 s was used for the coupling of this phosphoramidite. NMR samples were prepared by dissolving  $\sim 0.5 \mu\text{mol}$  of purified DNA samples into 500  $\mu\text{L}$  of buffer solution containing 150 mM sodium chloride, 10 mM sodium phosphate (pH 7.0), and 0.1 mM 2,2-dimethyl-2-silapentane-5-sulfonic acid (DSS).

**NMR Study.** All NMR experiments were performed using Bruker ARX-500, AV-500, and AV-700 spectrometers operating at 500.13, 500.30, and 700.21 MHz, respectively. For studying labile proton signals, the samples were prepared in a 90%  $\text{H}_2\text{O}$ /10%  $\text{D}_2\text{O}$  buffer solution. One-dimensional (1D) imino spectra were acquired using the water suppression by gradient-tailored excitation (WATERGATE) pulse sequence.<sup>45,46</sup> Two-dimensional (2D) WATERGATE-nuclear Overhauser effect spectroscopy (NOESY) was performed with a mixing time of 300 ms. In order to better observe the labile proton signals, some of these experiments were also repeated at temperatures below 25  $^\circ\text{C}$ . For studying nonlabile proton signals, the solvent was exchanged with a 100%  $\text{D}_2\text{O}$  buffer solution. 2D NOESY experiments were also performed with a mixing time of 300 ms and a data size of  $4096 \times 512$ . The acquired data sets were zero-filled to give  $4096 \times 4096$  spectra with a cosine window function applied to both dimensions. 2D double-quantum-filtered (DQF) correlation spectroscopy (COSY) was performed to show the scalar-coupled protons, and a sine window function was applied to both dimensions for measuring the vicinal  $J$ -couplings between  $\text{H1}'$  and  $\text{H2}'/\text{H2}''$  ( $^3J_{\text{H1}'\text{H2}'}$  and  $^3J_{\text{H1}'\text{H2}''}$ ).

For adenine H2 protons, the assignments were confirmed by  $^1\text{H}$ – $^{13}\text{C}$  heteronuclear multiple-bond correlation (HMBC) experiments<sup>47</sup> with an evolution period of 65 ms for the long-range couplings. The  $^{13}\text{C}$  spectral width was set to 60 ppm, and the carrier frequency was centered at 140 ppm. Backbone  $^{31}\text{P}$  signals were assigned using 2D total correlation spectroscopy (TOCSY) with a mixing time of 75 ms and  $^1\text{H}$ – $^{31}\text{P}$  heteronuclear single-quantum coherence (HSQC) experiments. The  $^{31}\text{P}$  spectral width was set to 4 ppm, and a data size of  $2048 \times 256$  was collected. 2D  $^1\text{H}$ – $^{31}\text{P}$  COSY experiments with a Gaussian inversion pulse centered at the H3' region were also performed, and  $2048 \times 128$  data sets were collected. The  $^{31}\text{P}$  dimension was extended to 180 complex points by forward linear prediction and zero-filled to 2048 complex points for measuring the heteronuclear  $J$ -coupling between H3' and  $^{31}\text{P}$  ( $^3J_{\text{H3}'\text{P}}$ ).  $^{13}\text{C}$  and  $^{31}\text{P}$  chemical shifts were indirectly referenced to DSS using the derived nucleus-specific ratio of 0.251 449 530 and 0.404 808 636, respectively.<sup>48</sup>

**Optical Melting Study.** For primer-template samples adopting a single conformation, ultraviolet absorbance data were measured from 25 to 95  $^\circ\text{C}$  at a heating rate of 0.8  $^\circ\text{C}/\text{min}$  using a Hewlett-Packard 8453 diode-array ultraviolet–visible spectrophotometer. The concentrations of samples were kept at 3  $\mu\text{M}$  in NMR buffer solution, and a 10 mm path length cuvette was used. Thermodynamic parameters were determined by fitting the melting curves using the absorbance data at 260 nm and the software MELTWIN 3.5 (available from Jeffrey A. McDowell at <http://www.meltwin3.com>).

## RESULTS AND DISCUSSION

In this study, we performed high-resolution NMR spectroscopic investigations focusing on 1D imino proton and 2D nuclear Overhauser effect (NOE) analyses to probe the replicating site structures of 5'-CX, 5'-GX, 5'-AX, and 5'-TX

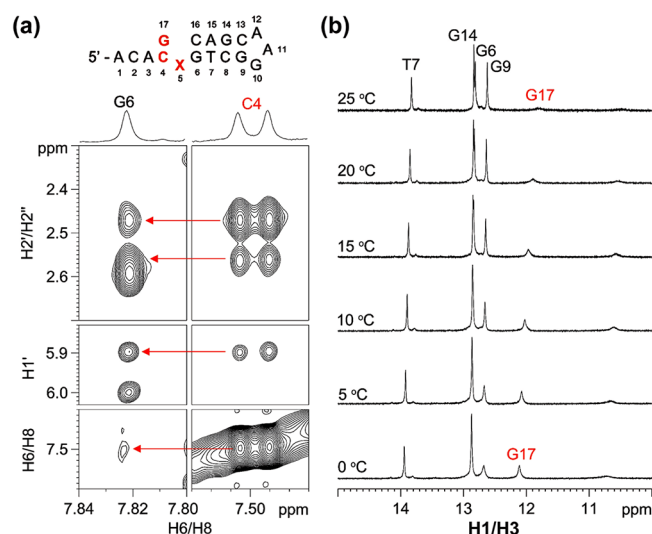


**Figure 2.** (a) For 5'-CX, the presence of unusual C4 H1'–G6 H8, C4 H2'/H2''–G6 H8, and C4 H6–G6 H8 NOEs (indicated by red arrows) supports the slipped structure. The inter-residue C4 H2'–G6 H8 NOE was partially overlapped with the intraresidue G6 H2'–G6 H8 NOE (the bottom cross peak in the top-left panel). (b) Variable temperature imino proton spectra of 5'-CX. The small and broad signal at ~10.7 ppm was contributed by the G·A sheared mispair of the GAA loop.

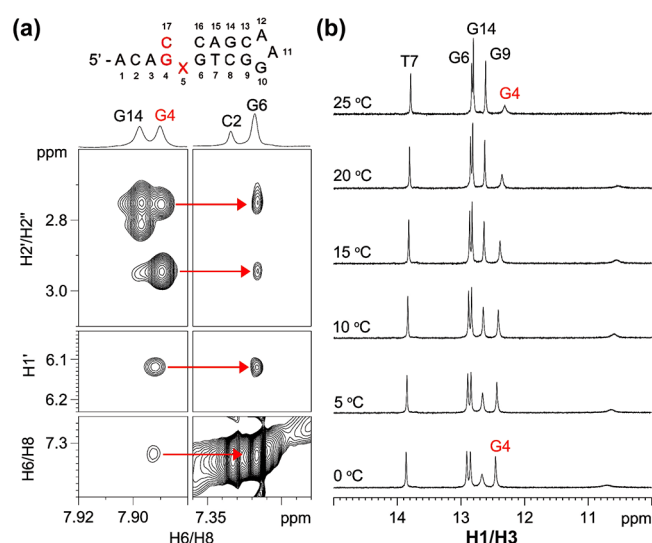


**Figure 3.** (a) For 5'-GX, the presence of unusual G4 H1'–G6 H8, G4 H2'/H2''–G6 H8, and G4 H8–G6 H8 NOEs (indicated by red arrows) supports the slipped structure. (b) Variable temperature imino proton spectra of 5'-GX.

primer-template models after the incorporation of dGTP, dCTP, dTTP, and dATP, respectively. Sequential assignments were made from the H6/H8–H1' fingerprint regions in 2D NOESY spectra in D<sub>2</sub>O and/or H<sub>2</sub>O (Supporting Information, S1–S4) using standard methods.<sup>49</sup> The assignment of adenine H2 was confirmed by HMBC experiments<sup>47</sup> (Supporting Information, S5). The successful coupling of the AP site was evidenced by the COSY cross peak between H1'/H1'' (~4.0 ppm) and H2'/H2'' (~2.2 ppm) of X5 (Supporting Information, S6). On the basis of the H3' assignment results from TOCSY, the backbone <sup>31</sup>P signals were assigned using <sup>1</sup>H–<sup>31</sup>P HSQC spectra (Supporting Information, S7). As

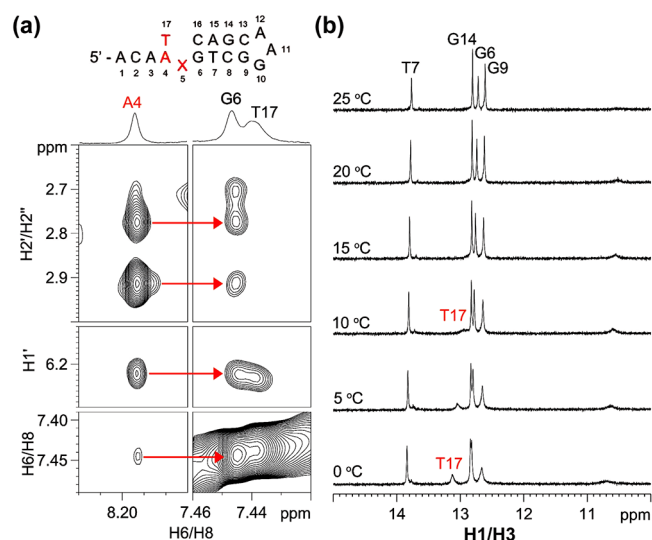


**Figure 4.** (a) For 5'-AX, the presence of unusual A4 H1'–G6 H8, A4 H2'/H2''–G6 H8, and A4 H8–G6 H8 NOEs (indicated by red arrows) supports the slipped structure. (b) Variable temperature imino proton spectra of 5'-AX.

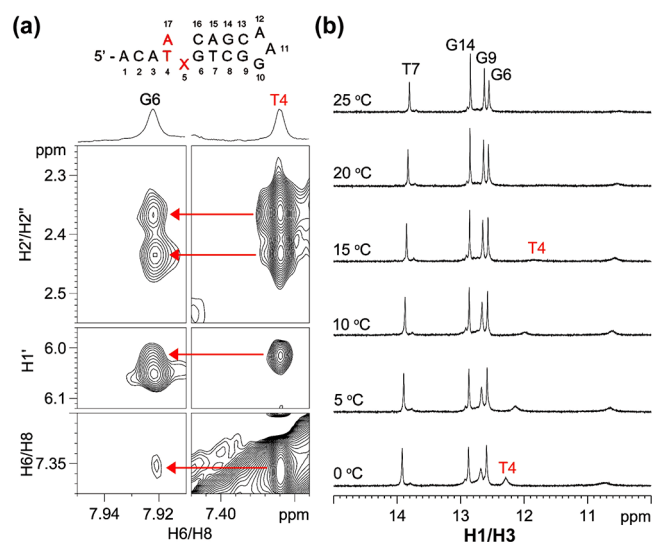


**Figure 5.** (a) For 5'-TX, the presence of unusual T4 H1'–G6 H8, T4 H2'/H2''–G6 H8, and T4 H8–G6 H8 NOEs (indicated by red arrows) supports the slipped structure. (b) Variable temperature imino proton spectra of 5'-TX.

revealed by the characteristic chemical shifts of the GAA loop,<sup>50</sup> including the broadened A12 H8 signal (~8.0 ppm) and the unusually upfield G9 H8 signal (~7.2 ppm) of the closing-loop base pair (Supporting Information, S1a–S4a), all primer-template models were found to adopt the designed hairpin conformation instead of forming homoduplexes and their proton chemical shifts were summarized in the Supporting Information, S8–S11.

**Replicating Site Structures of 5'-CX, 5'-GX, 5'-AX, and 5'-TX Models.** When a dGTP was incorporated opposite the AP site in the 5'-CX model, a misaligned primer-template structure was formed, as evidenced by the unusual NOEs between (i) C4 H1' and G6 H8, (ii) C4 H2'/H2'' and G6 H8, and (iii) C4 H6 and G6 H8 (Figure 2a), indicating C4 and G6 are close in space and stack on each other. This slipped structure was further supported by the formation of a G17·C4



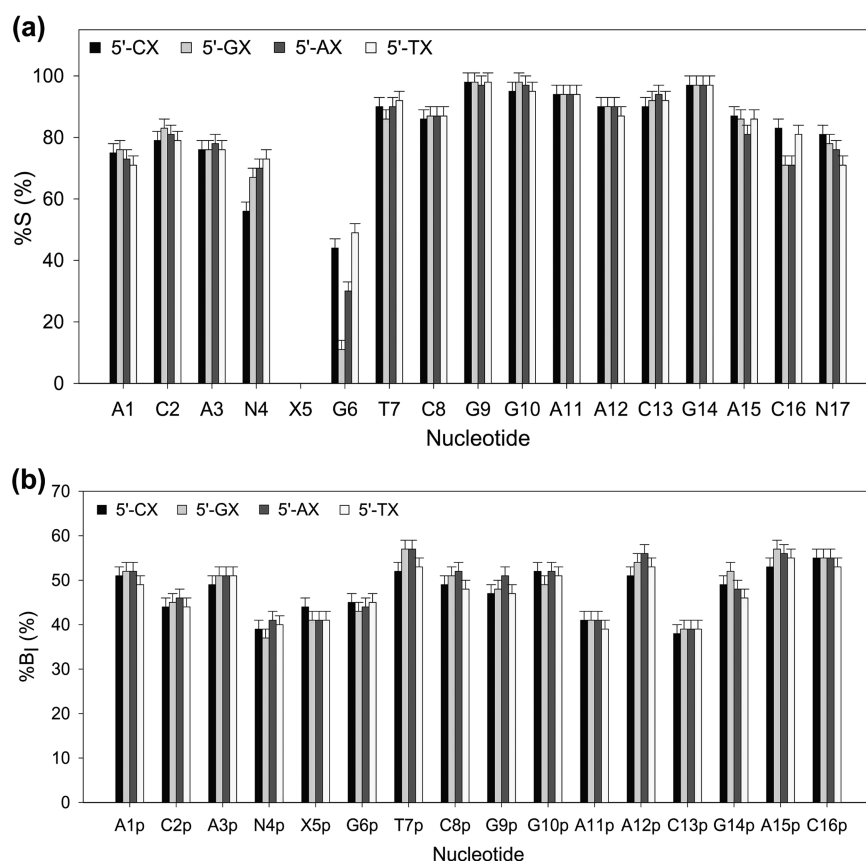


**Figure 6.** (a) The percentage of S-state sugar conformation and (b) the percentage population of B<sub>1</sub> backbone conformation of each residue in 5'-CX, 5'-GX, 5'-AX, and 5'-TX. The %S values of X5 were not determined due to complications in the splitting pattern of their H1'/H1''–H2'/H2'' COSY cross peaks.

Watson–Crick base pair, as indicated by the presence of a G17 imino signal (Figure 2b) and the NOEs between G17 imino and C4 amino protons (Supporting Information, S1b).

Similarly, after incorporation of a dCTP opposite the AP site in 5'-GX model, strand slippage was also observed. The incoming dCTP paired up with the upstream G4 instead of X5. This was supported by the unusual NOEs between (i) G4 H1' and G6 H8, (ii) G4 H2'/H2'' and G6 H8, and (iii) G4 H8 and G6 H8 (Figure 3a), showing G4 and G6 were close in space and X5 was slipped out. The appearance of a G4 imino signal (Figure 3b) and the NOEs between G4 imino and C4 amino protons (Supporting Information, S2b) indicate the formation of a G4–C17 Watson–Crick base pair, further supporting the formation of slipped structure.

For the 5'-AX model, a misaligned structure was also observed after a dTTP was incorporated opposite the AP site. As evidenced by the unusual NOEs between (i) A4 H1' and G6 H8, (ii) A4 H2'/H2'' and G6 H8, and (iii) A4 H8 and G6 H8 (Figure 4a), the incoming dTTP paired up with the upstream A4 instead of X5. The A4 H8–G6 H8 NOE reveals the favorable 5'-AG–3' purine–purine stack<sup>51</sup> which helps in stabilizing the misaligned structure. The appearance of T17 imino at lower temperatures (Figure 4b) and the NOE between T17 imino and A4 H2 NOE (Supporting Information, S3b) show the formation of a terminal T17–A4 base pair, confirming the formation of slipped structure.

As supported by the unusual NOEs between (i) T4 H1' and G6 H8, (ii) T4 H2'/H2'' and G6 H8, and (iii) T4 H6 and G6 H8 (Figure 5a), the incoming dATP was found to pair up with

the upstream T4 in 5'-TX model. Although the stabilizing effect from the T4–G6 stack was relatively weaker than the A4–G6 stack in 5'-AX,<sup>51</sup> the presence of the T4 imino signal at lower temperatures (Figure 5b) and the NOE between T4 imino and A17 H2 (Supporting Information, S4b) confirm the formation of a terminal A17–T4 Watson–Crick base pair, and thus the misaligned structure.

**Sugar Pucker and Backbone Conformation.** The effect of AP site on sugar pucker was studied by the percentage of S-state (%S) calculated from the sum of vicinal <sup>3</sup>J<sub>H1'H2'</sub> and <sup>3</sup>J<sub>H1'H2''</sub> coupling constants (Σ1').<sup>52</sup> The Σ1' values were measured from the H1'–H2'/H2'' cross peaks in DQF-COSY spectra at 25 °C (Supporting Information, S12). Except for the downstream G6, most residues adopted predominantly the S-state sugar conformation (Figure 6a). For 5'-CX and 5'-TX models in which a pyrimidine–purine stack was present in the misaligned structures, the %S values of G6 were found to be 44 and 49%, respectively. For 5'-GX and 5'-AX models in which a more favorable purine–purine stack<sup>51</sup> was present, the %S values of G6 were found to be only 11 and 30%, respectively. This suggests that the misaligned structures do not favor an S-state sugar downstream of the slipped out site.

For the backbone conformation, the effect of AP site was studied by the percentage population of B<sub>1</sub> conformation (%B<sub>1</sub>) calculated from the <sup>3</sup>J<sub>H3'P</sub> coupling constant.<sup>53</sup> The <sup>3</sup>J<sub>H3'P</sub> values were measured from the H3'–<sup>31</sup>P cross peaks in <sup>1</sup>H–<sup>31</sup>P COSY spectra (Supporting Information, S13). The %B<sub>1</sub> values of all residues in 5'-CX, 5'-GX, 5'-AX, and 5'-TX models were found to vary slightly between 38 and 55% (Figure 6b), indicating the

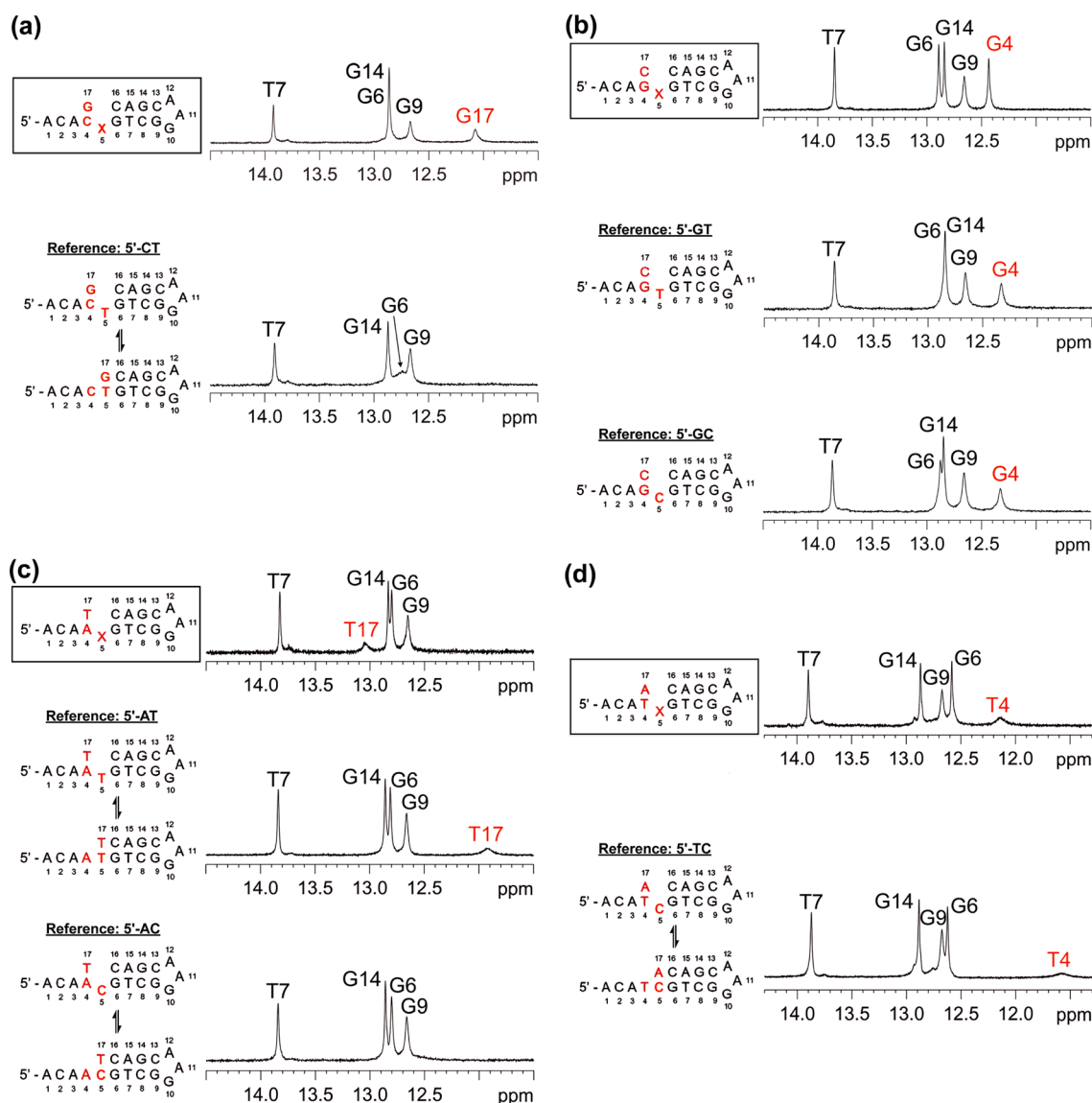


**Figure 7.** Imino proton spectra of (a) 5'-CX, (b) 5'-GX, (c) 5'-AX, and (d) 5'-TX and their corresponding reference sequences at 5 °C. The imino signals of the references were either broadened or not observed.

AP site has only a negligible effect on the backbone conformation of these primer-template models.

**Comparison of the Abasic Sites with Natural Templating Bases.** Recently, we have concluded that strand slippage can occur in any kind of natural templating bases during DNA replication,<sup>31</sup> providing insights into the origin of mutation hotspots in natural DNA sequences. The propensity of strand slippage was found to be higher in pyrimidine templates<sup>32–34</sup> than purine templates.<sup>30,31</sup> In addition, the slippage propensity was also found to relate to the type of terminal base pair formed in the primer-templates. In this work, misaligned structures were formed in all abasic templates with different types of upstream bases, suggesting strand slippage occurs in abasic primer-templates regardless of the type of terminal base pair formed.

In order to understand the effect of AP site on the propensity of strand slippage, we have compared the imino signals of the terminal base pairs formed in the abasic primer-template models with their corresponding reference samples that were shown to be capable of adopting a misaligned structure.<sup>30–34</sup>

Except for the replicating site, the sequences of these reference samples and the abasic primer-template models used in this study are the same. For the 5'-CX model, there was one reference sequence, namely, 5'-CT, that could be used for comparison.<sup>32,33</sup> At 5 °C, the half-height line width of G17 imino of the 5'-CX model was ~18 Hz (Figure 7a). Owing to the exchange between the misaligned and mismatched conformers, the G17 imino signal of 5'-CT was too broad to be observed. The line width difference suggests that base excision of the templating thymine favors the formation of the misaligned conformer, instead of the mismatched one. For the 5'-GX model, two reference sequences, namely, 5'-GT and 5'-GC, were found.<sup>32–34</sup> The G4 imino line width of 5'-GX was found to be ~10 Hz, whereas those of 5'-GT and 5'-GC were both ~20 Hz (Figure 7b). The narrower line width suggests the terminal G4:C17 base pair is more stable after the removal of the templating thymine or cytosine base. For the 5'-AX model, the T17 imino line width was ~27 Hz, whereas that of the reference 5'-AT was ~54 Hz (Figure 7c).<sup>32,33</sup> Owing to conformational exchange, the T17 imino of the other reference

5'-AC was too broad to be observed.<sup>34</sup> For the 5'-TX model, the T4 imino line width was ~45 Hz, whereas that of the reference 5'-TC was ~68 Hz (Figure 7d).<sup>34</sup> The narrower line width suggests that the removal of the templating base provides better stacking stabilization for the terminal base pair, and thus more stable misaligned structures in the abasic primer-template models.

As the two corresponding reference sequences of 5'-GX were found to adopt only a single misaligned conformer,<sup>32–34</sup> optical melting studies were performed to investigate the relative thermodynamic stabilities of these primer-template models. The results show that the abasic misaligned conformer was ~1 kcal/mol more stable than the corresponding references with a thymine or cytosine bulge (Supporting Information, S14), revealing the removal of the pyrimidine base in the bulge results in an improved G4–G6 stack which helps stabilize the misaligned conformation. Together with the narrower terminal imino line width, we conclude that the presence of an AP site in templates leads to a higher propensity of strand slippage in primer-templates.

**Biological Implications.** Together with our previous results on purines and pyrimidines,<sup>30–34</sup> strand slippage propensity due to the different types of templating residues was found to follow this order: abasic > pyrimidine > purine. The trend indicates that a smaller templating base will bring about a higher propensity of strand slippage in primer-templates, and thus a higher chance of expansion or deletion errors during DNA replication. Recently, enhanced levels of DNA repeat expansion were observed when BER of oxidized guanines occurred at or near CAG repeats.<sup>54,55</sup> Upon replacing a guanine within a CAG repeat bulge loop domain with an AP residue, the energetics proximal to and/or within the CAG repeat domains were altered and the population of slipped/looped DNA structures relative to the corresponding lesion-free construct was promoted.<sup>56</sup> Our current results suggest that the presence of an AP site in templates enhances strand slippage through the formation of a more stable misaligned structure during DNA replication, providing insights into the interplay between BER and triplet repeat expansion.

## CONCLUSIONS

In this study, we found that misaligned structures occur in primer-template models containing a templating abasic residue regardless of the type of terminal base pair formed. Owing to the improved stacking resulting from the removal of the base at the replicating site in misaligned primer-template models, we also found that abasic residues possess a higher propensity of strand slippage than natural templating bases.

## ASSOCIATED CONTENT

### Supporting Information

Figures and tables showing sequential NOE and imino assignments, <sup>1</sup>H–<sup>13</sup>C HMBC, DQF-COSY, and <sup>1</sup>H–<sup>13</sup>C HSQC spectra, summary of <sup>1</sup>H chemical shifts, Σ1' and %S, <sup>3</sup>J<sub>H3'P</sub> and %B<sub>I</sub> of 5'-CX, 5'-GX, 5'-AX, and 5'-TX, and thermodynamics of 5'-GX, 5'-GT, and 5'-GC. This material is available free of charge via the Internet at <http://pubs.acs.org>.

## AUTHOR INFORMATION

### Corresponding Author

\*Phone: (852) 3943-8126. Fax: (852) 2603-5057. E-mail: [lams@cuhk.edu.hk](mailto:lams@cuhk.edu.hk)

## Notes

The authors declare no competing financial interest.

## ACKNOWLEDGMENTS

We would like to thank Professors H. K. Lee, H. N. C. Wong, and J. C. Yu for their continuing support on the research activities of our group. The work described in this paper was supported by a General Research Fund (Project No. CUHK401308) and Special Equipment Grant (Project No. SEG/CUHK09) from the Research Grants Council of the Hong Kong Special Administrative Region.

## REFERENCES

- (1) Loeb, L. A.; Preston, B. D. *Annu. Rev. Genet.* **1986**, *20*, 201–230.
- (2) Lindahl, T. *Nature* **1993**, *362*, 709–715.
- (3) Srivastava, D. K.; Berg, B. J.; Prasad, R.; Molina, J. T.; Beard, W. A.; Tomkinson, A. E.; Wilson, S. H. *J. Biol. Chem.* **1998**, *273*, 21203–21209.
- (4) Nash, H. M.; Bruner, S. D.; Scharer, O. D.; Kawate, T.; Addona, T. A.; Spooner, E.; Lane, W. S.; Verdine, G. L. *Curr. Biol.* **1996**, *6*, 968–980.
- (5) Dizdaroğlu, M.; Karahalil, B.; Senturker, S.; Buckley, T. J.; Roldan-Arjona, T. *Biochemistry* **1999**, *38*, 243–246.
- (6) Wyatt, M. D.; Allan, J. M.; Lau, A. Y.; Ellenberger, T. E.; Samson, L. D. *Bioessays* **1999**, *21*, 668–676.
- (7) Nair, D. T.; Johnson, R. E.; Prakash, L.; Prakash, S.; Aggarwal, A. K. *J. Mol. Biol.* **2011**, *406*, 18–28.
- (8) Choi, J. Y.; Lim, S.; Kim, E. J.; Jo, A.; Guengerich, F. P. *J. Mol. Biol.* **2010**, *404*, 34–44.
- (9) Tippin, B.; Pham, P.; Goodman, M. F. *Trends Microbiol.* **2004**, *12*, 288–295.
- (10) Kunkel, T. A. *Cold Spring Harbor Symp. Quant. Biol.* **2009**, *74*, 91–101.
- (11) Fijalkowska, I. J.; Schaaper, R. M.; Jonczyk, P. *FEMS Microbiol. Rev.* **2012**, *36*, 1105–1121.
- (12) Friedberg, E. C.; Lehmann, A. R.; Fuchs, R. P. *Mol. Cell* **2005**, *18*, 499–505.
- (13) Yang, W. *FEBS Lett.* **2005**, *579*, 868–872.
- (14) Sale, J. E.; Lehmann, A. R.; Woodgate, R. *Nat. Rev. Mol. Cell Biol.* **2012**, *13*, 141–152.
- (15) Cuniassé, P.; Sowers, L. C.; Eritja, R.; Kaplan, B.; Goodman, M. F.; Cognet, J. A.; LeBret, M.; Guschlbauer, W.; Fazakerley, G. V. *Nucleic Acids Res.* **1987**, *15*, 8003–8022.
- (16) Shibutani, S.; Grollman, A. P. *J. Biol. Chem.* **1993**, *268*, 11703–11710.
- (17) Shibutani, S.; Takeshita, M.; Grollman, A. P. *J. Biol. Chem.* **1997**, *272*, 13916–13922.
- (18) Daube, S. S.; Arad, G.; Livneh, Z. *Biochemistry* **2000**, *39*, 397–405.
- (19) Lin, Z.; Hung, K. N.; Grollman, A. P.; de los Santos, C. *Nucleic Acids Res.* **1998**, *26*, 2385–2391.
- (20) Cuniassé, P.; Sowers, L. C.; Eritja, R.; Kaplan, B.; Goodman, M. F.; Cognet, J. A.; LeBret, M.; Guschlbauer, W.; Fazakerley, G. V. *Biochemistry* **1989**, *28*, 2018–2026.
- (21) Cuniassé, P.; Fazakerley, G. V.; Guschlbauer, W.; Kaplan, B. E.; Sowers, L. C. *J. Mol. Biol.* **1990**, *213*, 303–314.
- (22) Kalnik, M. W.; Chang, C. N.; Grollman, A. P.; Patel, D. J. *Biochemistry* **1988**, *27*, 924–931.
- (23) Kalnik, M. W.; Chang, C. N.; Johnson, F.; Grollman, A. P.; Patel, D. J. *Biochemistry* **1989**, *28*, 3373–3383.
- (24) Withka, J. M.; Wilde, J. A.; Bolton, P. H.; Mazumder, A.; Gerlt, J. A. *Biochemistry* **1991**, *30*, 9931–9940.
- (25) Goljer, I.; Kumar, S.; Bolton, P. H. *J. Biol. Chem.* **1995**, *270*, 22980–22987.
- (26) Singh, M. P.; Hill, G. C.; Peoc'h, D.; Rayner, B.; Imbach, J. L.; Lown, J. W. *Biochemistry* **1994**, *33*, 10271–10285.
- (27) Coppel, Y.; Berthet, N.; Coulombeau, C.; Coulombeau, C.; Garcia, J.; Lhomme, J. *Biochemistry* **1997**, *36*, 4817–4830.

- (28) Chen, J.; Dupradeau, F. Y.; Case, D. A.; Turner, C. J.; Stubbe, J. *Nucleic Acids Res.* **2008**, *36*, 253–262.
- (29) Chen, J.; Dupradeau, F. Y.; Case, D. A.; Turner, C. J.; Stubbe, J. *Biochemistry* **2007**, *46*, 3096–3107.
- (30) Chi, L. M.; Lam, S. L. *Biochemistry* **2009**, *48*, 11478–11486.
- (31) Chi, L. M.; Lam, S. L. *J. Phys. Chem. B* **2012**, *116*, 1999–2007.
- (32) Chi, L. M.; Lam, S. L. *FEBS Lett.* **2006**, *580*, 6496–6500.
- (33) Chi, L. M.; Lam, S. L. *Biochemistry* **2007**, *46*, 9292–9300.
- (34) Chi, L. M.; Lam, S. L. *Biochemistry* **2008**, *47*, 4469–4476.
- (35) Panigrahi, G. B.; Cleary, J. D.; Pearson, C. E. *J. Biol. Chem.* **2002**, *277*, 13926–13934.
- (36) Kang, S.; Jaworski, A.; Ohshima, K.; Wells, R. D. *Nat. Genet.* **1995**, *10*, 213–218.
- (37) Yoshizawa, S.; Kawai, G.; Watanabe, K.; Miura, K.; Hirao, I. *Biochemistry* **1997**, *36*, 4761–4767.
- (38) Weiss, B.; Grossman, L. *Adv. Enzymol. Relat. Areas Mol. Biol.* **1987**, *60*, 1–34.
- (39) Randall, S. K.; Eritja, R.; Kaplan, B. E.; Petruska, J.; Goodman, M. F. *J. Biol. Chem.* **1987**, *262*, 6864–6870.
- (40) Takeshita, M.; Chang, C. N.; Johnson, F.; Will, S.; Grollman, A. P. *J. Biol. Chem.* **1987**, *262*, 10171–10179.
- (41) Takeuchi, M.; Lillis, R.; Demple, B.; Takeshita, M. *J. Biol. Chem.* **1994**, *269*, 21907–21914.
- (42) Wilson, D. M., III; Takeshita, M.; Grollman, A. P.; Demple, B. J. *Biol. Chem.* **1995**, *270*, 16002–16007.
- (43) Paz-Elizur, T.; Takeshita, M.; Goodman, M.; O'Donnell, M.; Livneh, Z. *J. Biol. Chem.* **1996**, *271*, 24662–24669.
- (44) Paz-Elizur, T.; Takeshita, M.; Livneh, Z. *Biochemistry* **1997**, *36*, 1766–1773.
- (45) Piotto, M.; Saudek, V.; Sklenar, V. *J. Biomol. NMR* **1992**, *2*, 661–665.
- (46) Sklenar, V.; Piotto, M.; Leppik, R.; Saudek, V. *J. Magn. Reson., Ser. A* **1993**, *102*, 241–245.
- (47) van Dongen, M. J.; Wijmenga, S. S.; Eritja, R.; Azorin, F.; Hilbers, C. W. *J. Biomol. NMR* **1996**, *8*, 207–212.
- (48) Markley, J. L.; Bax, A.; Arata, Y.; Hilbers, C. W.; Kaptein, R.; Sykes, B. D.; Wright, P. E.; Wuthrich, K. *Pure Appl. Chem.* **1998**, *70*, 117–142.
- (49) Wijmenga, S. S.; van Buuren, B. N. M. *Prog. Nucl. Magn. Reson. Spectrosc.* **1998**, *32*, 287–387.
- (50) Hirao, I.; Kawai, G.; Yoshizawa, S.; Nishimura, Y.; Ishido, Y.; Watanabe, K.; Miura, K. *Nucleic Acids Res.* **1994**, *22*, 576–582.
- (51) Jafilan, S.; Klein, L.; Hyun, C.; Florian, J. *J. Phys. Chem. B* **2012**, *116*, 3613–3618.
- (52) van Wijk, J.; Huckriede, B. D.; Ippel, J. H.; Altona, C. *Methods Enzymol.* **1992**, *211*, 286–306.
- (53) Gorenstein, D. G. *Chem. Rev.* **1994**, *94*, 1315–1338.
- (54) Kovtun, I. V.; Liu, Y.; Bjoras, M.; Klungland, A.; Wilson, S. H.; McMurray, C. T. *Nature* **2007**, *447*, 447–452.
- (55) McMurray, C. T. *DNA Repair* **2008**, *7*, 1121–1134.
- (56) Volker, J.; Plum, G. E.; Klump, H. H.; Breslauer, K. J. *J. Am. Chem. Soc.* **2009**, *131*, 9354–9360.